Talanta 146 (2016) 470–476

Contents lists available at ScienceDirect

Talanta

journal homepage: www.elsevier.com/locate/talanta

A colorimetric biosensor for detection of attomolar microRNA with a functional nucleic acid-based amplification machine

Dandan Li [a], Wei Cheng [b], Yurong Yan [a], Ye Zhang [a], Yibing Yin [a], Huangxian Ju [a,c,*], Shijia Ding [a,**]

[a] Key Laboratory of Clinical Laboratory Diagnostics (Ministry of Education), College of Laboratory Medicine, Chongqing Medical University, Chongqing 400016, China
[b] Molecular Oncology and Epigenetics Laboratory, the First Affiliated Hospital of Chongqing Medical University, Chongqing 400016, China
[c] State Key Laboratory of Analytical Chemistry for Life Science, School of Chemistry and Chemical Engineering, Nanjing University, Nanjing 210093, China

ARTICLE INFO

Article history:
Received 15 June 2015
Received in revised form
30 August 2015
Accepted 6 September 2015
Available online 8 September 2015

Keywords:
Colorimetric biosensing
Signal amplification
Toehold initiated rolling circle amplification
DNAzyme
MicroRNA

ABSTRACT

A functional nucleic acid-based amplification machine was designed for simple and label-free ultrasensitive colorimetric biosensing of microRNA (miRNA). The amplification machine was composed of a complex of trigger template and C-rich DNA modified molecular beacon (MB) and G-rich DNA (GDNA) as the probe, polymerase and nicking enzyme, and a dumbbell-shaped amplification template. The presence of target miRNA triggered MB mediated strand displacement to cyclically release nicking triggers, which led to a toehold initiated rolling circle amplification to produce large amounts of GDNAs. The formed GDNAs could stack with hemin to form G-quadruplex/hemin DNAzyme, a well-known horseradish peroxidase (HRP) mimic, for catalyzing a colorimetric reaction. The modified MB improved the stringent target recognition and reduced background signal. The proposed sensing strategy showed very high sensitivity and selectivity with a wide dynamic range from 10 aM to 1.0 nM, and enabled successful visual analysis of trace amount of miRNA in real sample by the naked eye. This rapid and highly efficient signal amplification strategy provided a simple and sensitive platform for miRNA detection. It would be a versatile and powerful tool for clinical molecular diagnostics.

1. Introduction

MicroRNAs (miRNAs) are short (18–23 nucleotides), endogenous, single-stranded RNA molecules that regulate the expression of mRNA in many cellular processes [1–3]. Since the discovery of miRNAs in circulation, large amounts of miRNA-related biological studies have confirmed that the dysregulated expression of miRNAs contributes to the pathogenesis of most human malignancies [4–8]. Therefore, miRNAs have been emerged as novel biomarkers in the diagnosis and treatment of cancers [9–11], which calls for rapid, simple, reliable, sensitive and selective assays for miRNAs detection.

Generally, northern blot and real-time PCR have been widely used for analysis of miRNA expression [12–14]. Though these methods have showed some merits, they still suffer from some drawbacks in practical applications, i.e., semi-quantitative, laborious, and requiring expensive equipment [15–16]. Hence, biosensing strategies, including electrochemical biosensors, luminescence sensors and colorimetric sensors, have become a class of powerful tools for accurate and quantitative miRNA expression [17–19]. Among them, colorimetric sensors have recently gained special attention due to the extreme simplicity and the visual detection of miRNAs in homogeneous solution without any separation and washing steps.

To improve the analytical performance of biosensing strategies, various amplification strategies, including exonuclease (Exo)-assisted signal amplification [20–21], strand displacement amplification (SDA) [22] and rolling circle amplification (RCA) [23–28] have been developed. Among these methods, RCA has received particular interest and has been widely used for the development of ultrasensitive biosensors. Though RCA has excellent property of signal amplification, it is apt to generate nonspecific amplification due to the impurity of circular template. Also, RCA products are large fragment of ssDNAs, which decreases the solubility and greatly increases the steric hindrance to hinder their hybridization with probe. All of these features may counteract the specificity of amplification methods based on RCA and compromise the analytical performance.

* Corresponding author at: Key Laboratory of Clinical Laboratory Diagnostics (Ministry of Education), College of Laboratory Medicine, Chongqing Medical University, Chongqing 400016, China. Fax: +86 25 83593593.
** Corresponding author.
E-mail addresses: hxju@nju.edu.cn (H. Ju), dingshijia@163.com (S. Ding).

http://dx.doi.org/10.1016/j.talanta.2015.09.010
0039-9140/

Aiming at improving the analytical performance of RCA-based amplification strategies for miRNAs detection, this work designed a complex of trigger template and C-rich DNA co-modified molecular beacon (MB) and G-rich DNA (GDA) as a probe, and integrated the MB mediated SDA with toehold initiated rolling circle amplification (TIRCA) to design a novel functional nucleic acid-based amplification machine for specific and ultrasensitive detection of miRNAs. Here, the amplification machine contained the MB/GDNA probe, polymerase and nicking enzyme, and a dumbbell-shaped amplification template as seal probe. The recognition of MB/GDNA probe with target miRNA triggered the MB mediated SDA to cyclically release nicking triggers, which then hybridized with the seal probe to trigger multiple TIRCA and produce large amounts of GDNAs. Specifically, the 3′-OH of MB and GDNA were inactivated by C6 spacer, which could decrease the nonspecific polymerization along with 5′ protruding termini of MB, thus improving the stringent target recognition and reducing background signal. In addition, the same specific nicking site recognized by Nb.BbvCI was sequestered in the modified MB and seal probe, which enabled only one nicking endonuclease being used to simplify the whole miRNA detection process. Also, it made sure that TIRCA products could be nicked to large amounts small fragments, which reduced the steric hindrance and facilitated solution of TIRCA products, resulting in greatly increased sensitivity.

The functional nucleic acid-based amplification machine produced large amounts of GDNA to form DNAzyme, a horseradish peroxidase (HRP) mimic [29–31]. The formed DNAzyme could catalyze the conversion of a colorless 2,2′-azino-bis(3-ethylbenzothiazoline-6-sulfonic acid) ($ABTS^{2-}$) to a green $ABTS^{\cdot -}$, and thus led to an ultrasensitive visual method for detection of miRNAs. Due to the presence of nicking enzyme and the nicking site in the seal probe, the amplification machine allowed the input of target miRNA to be converted to multiple outputs of DNAzyme, thus produced a mass of green $ABTS^{\cdot -}$ for ultrasensitive colorimetric and visual detection of miRNAs. This signal amplification and biosensing method provided a simple, rapid and sensitive platform for miRNA detection and could become a versatile tool for clinical molecular diagnostics.

2. Experimental

2.1. Materials and reagents

Phi29 DNA polymerase, Nb.BbvCI, T4 DNA ligase, dNTP, Exo-I, Exo-III and RNase inhibitor were purchased from New England Biolabs (USA). Hemin and $ABTS^{2-}$ were obtained from Sigma-Aldrich (St Louis, MO, USA). MiRNAs were obtained from TaKaRa Biotech. Inc. (Dalian, China). HPLC-purified DNA oligonucleotides were synthesized by Sangon Biotechnology Co. Ltd. (Shanghai, China). The sequences of nucleic acids employed in this study were shown in Table 1. All oligonucleotides were dissolved in tris-ethylenediaminetetraacetic acid (TE) buffer (pH 8.0, 10 mM Tris–HCl, 1 mM EDTA) and stored at −20 °C, which were diluted in appropriate buffer prior to use.

The stock solution of 1.0 μg/μL total RNA extracted from breast adenocarcinoma (MCF-7) cells was purchased from Ambion (California, USA). All solutions and deionized water used were treated with diethyprocarbonated (DEPC) and autoclaved to protect from RNase degradation. All aqueous solutions were prepared using Millipore-Q water (≥ 18 MΩ, Milli-Q, Millipore). The stock solution of hemin (5 mM) was diluted to the required concentrations with 25 mM 4-(2-hydroxyethyl)-1-piperazineëthanesulfonic acid (HEPES) (pH 8.0) containing 20 mM KCl, 200 mM NaCl, 0.05% Triton X-100 and 1% dimethyl sulfoxide (DMSO).

2.2. Apparatus

A UV-visible spectrophotometer (UV-2550, Shimadzu, Kyoto, Japan) was used to collect the signal. The gel electrophoresis was performed on the DYY-6C electrophoresis analyzer (Liuyi Instrument Company, China) and imaged on a Bio-rad ChemDoc XRS (Bio-Rad, USA). The concentrations of DNA suspensions were measured by ultraviolet spectrophotometry using a NanoDrop 1000 spectrophotometer (Thermo Scientific, Wilmington, DE, USA).

2.3. Preparation of MB/GDNA and seal probes

The MB/GDNA probe was prepared by simply mixing MB and GDNA at a ratio of 1.2:1 to incubate at room temperature (RT) for 1 h. The resulting hybridization complex was stored at −20 °C before use. Seal probe was prepared by self-templated ligation of 5′-phosphorylated dumbbell-shaped DNA sequence using T4 DNA ligase. The ligation reaction was conducted in a 20-μL reaction mixture containing 1 × T4 DNA ligase reaction buffer (50 mM Tris–HCl, 10 mM $MgCl_2$, 1 mM ATP, 10 mM dithiothreitol, pH 7.5), 1 μL DNA seal probes (100 μM), 17 μL DEPC-treated H_2O and 100 U of T4 DNA ligase. Ligation process was performed at 16 °C overnight and followed by inactivation at 65 °C for 10 min to terminate the ligation reaction. After ligation, Exo-III (100 U/μL) and Exo-I (20 U/μL) were added to digest the leftover dsDNA and ssDNA to yield closed DNA. Following digestion, the Exos were denatured by heating at 80 °C for 20 min. These prepared probe was then stored at −20 °C until use.

2.4. Signal measurement

0.5 μL of target miRNA or sample was added in 100 μL mixture of 1 μM MB/GDNA probe, 0.2 U/μL Phi29 DNA polymerase, 0.15 U/

Table 1
Nucleic acids employed in the present work.

Nucleic acid[a]	Sequence (5′-3′)[b]
miRNA21	UAGCUUAUCAGACUGAUGUUGA
miRNA222	AGCUACAUCUGGCUACUGGGUCUC
SM	UAGCUUAUCAGACUGAUGUUUA
DM	UAGCUUAUCAGACUGAUUUUUA
NC	AUUGAAUAUUCUUAUUAUAAUU
MB	GTCAGATGAATTCGTGTGAGAGCACCTCAGCAACCCGCCCAACGCGCGTCAACATCAGTCTGATAAGCTAGACGCGCG – C6 SPACER
GDNA	GGGTTGGGCGGGTTGGG – C6 SPACER
Seal probe	GTGAGAGCCCAACCCGCCCTACCCTAGACCTCAGCTCTCACACGAATTCCCGTCAGATGAATTCGT

[a] SM, single-base mismatched strand; DM, double-base mismatched strand; NC, non-complementary mismatched strand; MB, trigger template and C-rich DNA modified molecular beacon with C6 SPACER protected 3′-end.
[b] The colors correspond to the sequences shown in Fig. 1.

μL Nb.BbvCI, 200 μM dNTP, 100 ug/L BSA, 1 U/μL RNase inhibitor, 10 μL phi29 DNA polymerase reaction buffer (500 mM Tris–HCl, 100 mM $MgCl_2$, 100 mM $(NH_4)_2SO_4$, and 40 mM DTT) and 10 μL CutSmart™ Buffer (500 mM potassium acetate, 20 mM Tris-acetate, 10 mM magnesium acetate, and 100 μg/ml BSA). After the resulting reaction mixture was incubated at 37 °C for 45 min, 500 ng/μL seal probe was added in the mixture to incubate at 37 °C for another 45 min. Afterward 260 μL HEPES buffer and 3 μL of hemin (200 μM) were added and incubated at RT for another 30 min to form DNAzyme.

130 μL of 8 mM $ABTS^{2-}$ and 32.5 μL of 32 mM H_2O_2 as the DNAzyme substrate were added to the reaction mixture and incubated at RT for 5 min. The absorbance of the mixture was then measured using a UV–vis absorption spectrophotometer in the wavelength range from 500 to 400 nm against a blank. The reaction rate was monitored at 418 nm.

2.5. Gel electrophoresis

The product of MB/GDNA hybridization was analyzed by 12% native polyacrylamide gel electrophoresis (PAGE) in 1 × TBE buffer (89 mM Tris–boric acid, 2 mM EDTA, pH 8.3) at a 110 V constant voltage for 60 min at 4 °C before staining with Goldview (Saibaisheng, China). The products of ligation reaction (non-ligated seal probe, non-digested seal probe, and prepared seal probe) were analyzed by agarose gel electrophoresis in 1 × TBE buffer at 120 V constant voltage for 25 min. The gels were visualized via gel image system (Bio-Rad Laboratories, USA).

3. Results and discussion

3.1. Principle of functional nucleic-based amplification machine

The principle of the functional nucleic acid-based amplification machine for miRNA detection is illustrated in Scheme 1. The MB template consists of four domains: a miRNA-recognition domain (a), a GDNA hybridization domain (b), an amplification domain for producing the nicking triggers (c) and a nicking domain for Nb.BbvCI recognition. The amplification domain is designed for SDA, which produces the nicking triggers to initiate the following TIRCA by hybridization with the seal probe.

In the presence of target miRNA, the specific hybridization of miRNA with domain (a) opens the circular part of MB, and the bound miRNA is extended along domain (b) and domain (c) to form a complete duplex with the aid of Ph29 DNA polymerase, which displaces the GDNA at domain b. Subsequently, the Nb.BbvCI specifically recognizes the duplex nicking site to cleave the extended DNA strand at domain (c), which is released as the nicking trigger. Upon the circulation of the extension and cleavage processes at domain (c), large amounts of nicking triggers are released as the primer to anneal with the seal probe to trigger the TIRCA.

Primarily, the seal probe remains stable as a dumbbell-shaped structure, which is blocked for RCA. Once the trigger is bound to the toehold domain of seal probe, the spontaneous branch migration leads to an activated circular form, thereby initiating the RCA. Due to the presence of the nicking site in the circle, the resultant DNA duplex can be cleaved by Nb.BbvCI and then further extended by Ph29 DNA polymerase, thus yielding hundreds of tandem repeats of GDNA. As a result, the amplified colorimetric detection is achieved by the formation of DNAzyme in the presence of hemin.

3.2. Characterization of probe preparation

The preparation of seal probes was firstly examined with agarose gel electrophoresis (Fig. 1A). The ligation product (Fig. 1A, lane b) remained the band of seal probe precursor (Fig. 1A, lane a). This band (Fig. 1A, lane c) also occurred after digestion with Exo-III and Ex-I, indicating the formation of closed seal probe. Otherwise the dsDNA with a recessed 3′-termini and the ssDNA would be digested by Exo-III and Exo-I, respectively. To verify whether miRNA and MB/GDNA probe could proceed as designed, PAGE analysis was carried out (Fig. 1B). The mixture of MB and GDNA showed two bands (Fig. 1B, lane e) at two positions different from MB (Fig. 1B, lane c) and GDNA (Fig. 1B, lane d), which resulted from the hybridization of MB with GDNA (MB/GDNA complexes), leading to a new band. After hybridization of the MB/GDNA probe with miRNA, a new band corresponding to the hybridization product was observed (Fig. 1B, lane f), revealing that the MB/GDNA probe was carried out as expected.

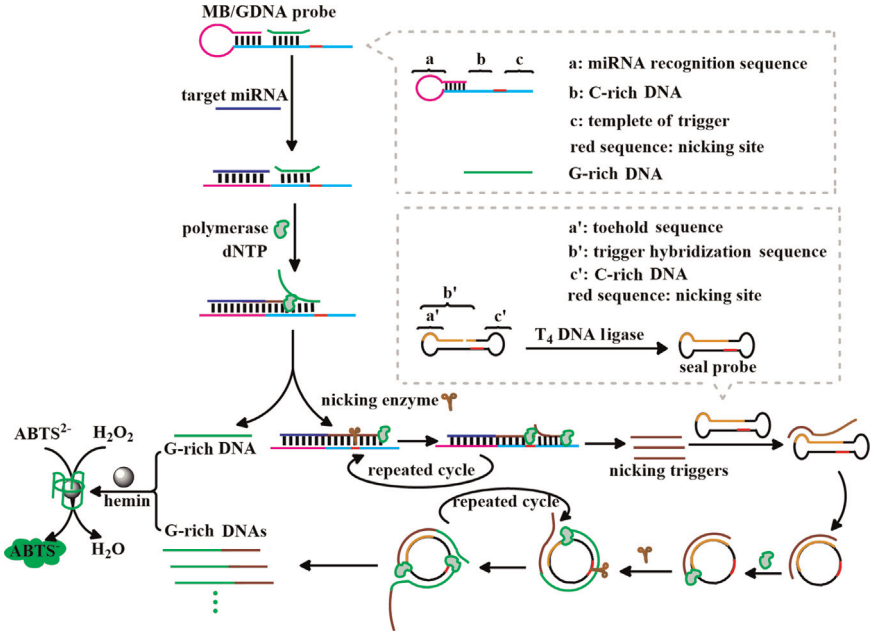

Scheme 1. Schematic illustration of functional nucleic acid-based amplification machine for miRNA detection.

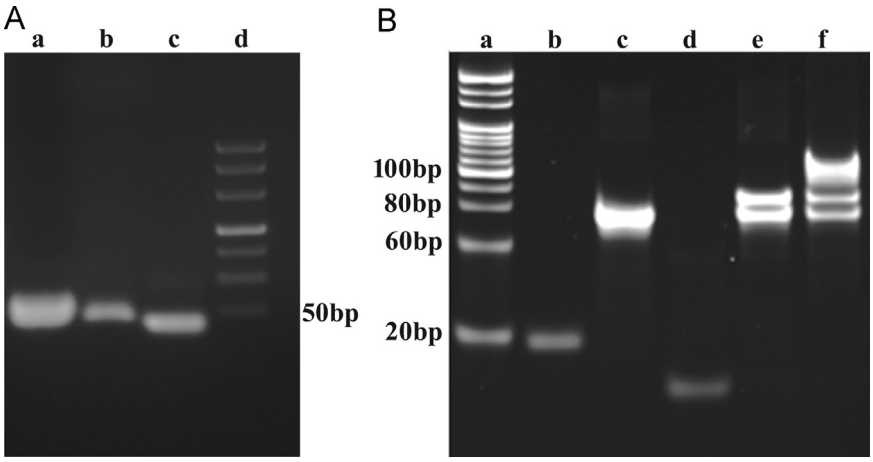

Fig. 1. (A) Agarose gel electrophoresis of seal probe precursor (a), seal probe before (b) and after (c) digestion with Exo-I and Exo-III, and DNA size marker (d), and (B) The native PAGE analysis: DNA size marker (a), miRNA (b), MB (c), Synthetic GDNA (d), complex of MB/GDNA probe (e) and the hybridization of miRNA with MB/GDNA probe loop (f).

3.3. Optimization of probe preparation and detection conditions

Owing to the breathing adjacent to the termini of helices, the formed MB/GDNA duplexes might be involved in strand melt, which resulted in the formation of DNAzyme via the binding of hemin with released GDNA to produce high background. Thus the ratio of MB to GDNA was firstly optimized. As shown in Fig. 2A, the $(A_1-A_2)/A_1$ value increased with the increasing ratio of MB to GDNA and then decreased at a ratio of 1.2:1. Here A_1 is the absorbance of $ABTS^{\cdot -}$ produced in the presence of DNAzyme, which was formed by the binding of hemin with GDNA used for preparation of the probe, A_2 is the absorbance of $ABTS^{\cdot -}$ produced in the presence of hemin and the reaction mixture of GDNA and MB, and the maximum $(A_1-A_2)/A_1$ value represents the lowest relative background signal. To further verify the MB-to-GDNA ratio, PAGE was used to analyze the optimization process. The bands of MB/GDNA complexes moved slower than MB and GDNA (Fig. 2B), which was similar to Fig. 1B (lane e), indicating the formation of MB/GDNA duplexes. Furthermore, ImageJ 1.48 software was used to verify the intensity of these bands, which showed the saturation at a ratio of 1.2:1. Thus the ratio of 1.2 for MB and GDNA was selected for the probe preparation.

To achieve an excellent analytical performance, some detection conditions, e.g. the concentration of Nb.BbvCI, reaction temperature and reaction time, were optimized at 100 pM miRNA (Fig. 3A–C). The absorbance of finally produced $ABTS^{\cdot -}$ increased dramatically with the increasing amount of Nb.BbvCI and kept constant after the concentration of 0.15 U/μL (Fig. 3A). Therefore, 0.15 U/μL of Nb.BbvCI was used in further experiments. The effect of the reaction temperature on the machine performance was evaluated in Fig. 3B, which showed the maximum absorbance at 37 °C. At the optimal reaction temperature, the effects of reaction time on both SDA and TIRCA were examined using the dependence of the absorbance of finally produced $ABTS^{\cdot -}$ on the total time with an equal time for two steps (Fig. 3C). The absorbance increased and then trended to a maximum value at the total time of 90 min, which was selected as the optimal reaction time.

3.4. Biosensing performance of the designed amplification machine

Under the optimal detection conditions, the UV–vis absorption increased with the increasing concentration of miRNA (Fig. 4A). The plot of the response vs. the logarithm of miRNA concentration showed a good linear relationship in the range from 10 aM to 1 nM with a correlation coefficient of 0.994 (insets in Fig. 4B). The linear range was much wider than that in the absence of TIRCA (the insets in Fig. 4C). According to the sum of blank response and 3 times standard deviation (3σ, $n=10$), the detection limit was calculated to be 5 aM, which was much lower than 10 pM for that without TIRCA, suggesting that the proposed amplification machine enabled ultrasensitive detection of miRNA. In the amplification machine the contribution of TIRCA could be further demonstrated from the readout difference between SDA amplification and SDA cascade TIRCA amplification in miRNA-21 detection (Fig. 4D). The detection limit of 5 aM was much better than those with flurescent [21,26,28,32], electrochemical [25] and

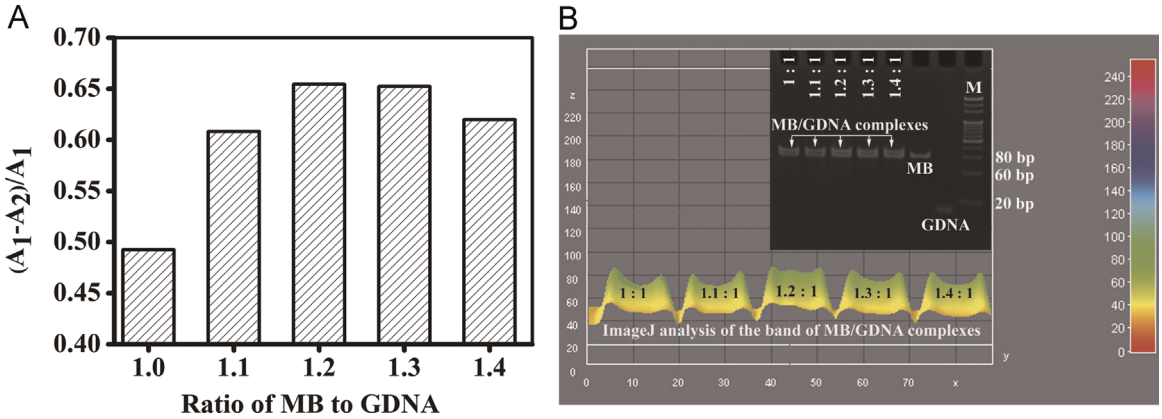

Fig. 2. Optimization of ratio of MB to GDNA (A) and corresponding PAGE analysis (B).

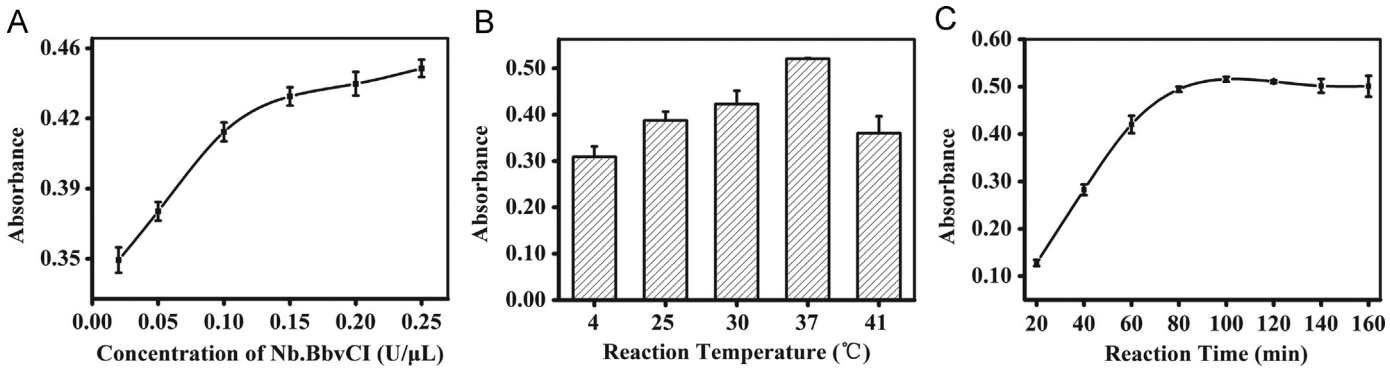

Fig. 3. Optimization of (A) Nb.BbvCI concentration, (B) reaction temperature (°C) and (C) reaction time (min). When one parameter changed the others were under their optimal conditions.

colorimetric [17,20,33] detection. Moreover, the color difference between the blank and the sample at 10 aM miRNA-21 could be well distinguished with the naked eye (inset in Fig. 4A), providing a simple and ultrasensitive visual method for miRNA detection.

3.5. Specificity and reproducibility of the designed method

As the Gibbs free energy (ΔG) of nucleic acid hybridization depends on salt concentration and temperature, the specific hybridization was investigated at diverse salt concentrations (including 10 mM Mg^{2+}, 12.5 mM Mg^{2+} and 300 mM Na^{+}) and temperatures (including 4 °C, 25 °C, 37 °C and 41 °C). According to the PAGE results, the hybridization of target miRNA-21 with MB at different salt concentrations (lanes 1, 6 and 8 in Fig. 5A) or temperatures (lanes 2, 7 10 and 12 in Fig. 5B) led to significant new band, while the hybridization of SM with MB showed much weaker bands in Fig. 5A (lanes 3, 7 and 9) and Fig. 5B (lanes 3, 8, and 11). Additionally, no new band was generated in lanes corresponding to MB spiked with DM, NC and miRNA-222. These results suggested that the salt concentration and temperature did not obviously influence the specificity of the developed strategy.

The specificity of the functional nucleic-based amplification

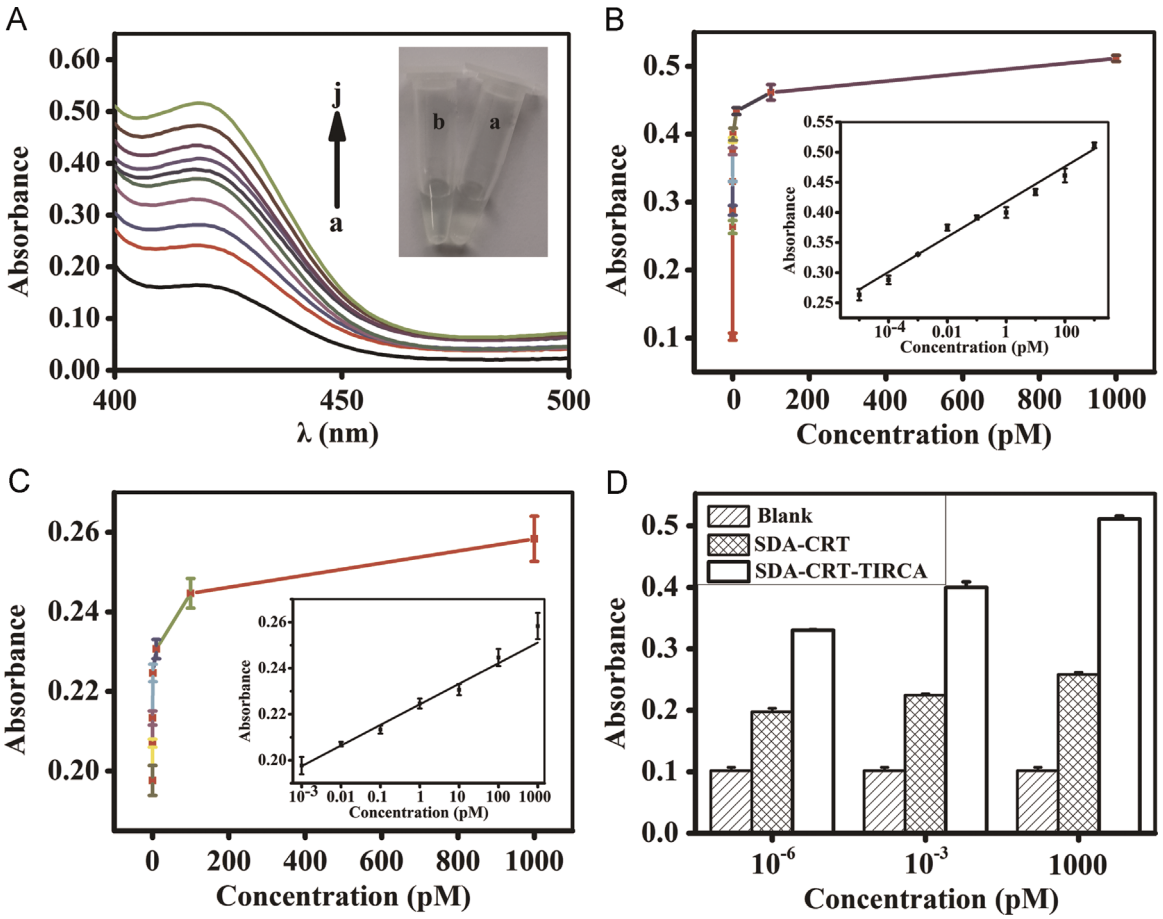

Fig. 4. (A) UV-visable spectra of DNAzyme substrate mixed with the reaction mixtures obtained at 0, 1×10^{-17}, 1×10^{-16}, 1×10^{-15}, 1×10^{-14}, 1×10^{-13}, 1×10^{-12}, 1×10^{-11}, 1×10^{-10} and 1×10^{-9} M miRNA-21 (a–j). Inset: photo of the final reaction solutions at 0 (a) and 10 aM miRNA-21 (b). (B) Plot of absorbance vs. miRNA-21 concentration. (C) Plot of absorbance vs. miRNA-21 concentration in the absence of TIRCA. Insets in (B) and (C): plots of the response vs. the logarithm of miRNA concentration. (D) Absorbance at three miRNA-21 concentrations with SDA amplification and SDA-TIRCA amplification. Error bars are the standard deviations of measurements taken from three independent experiments.

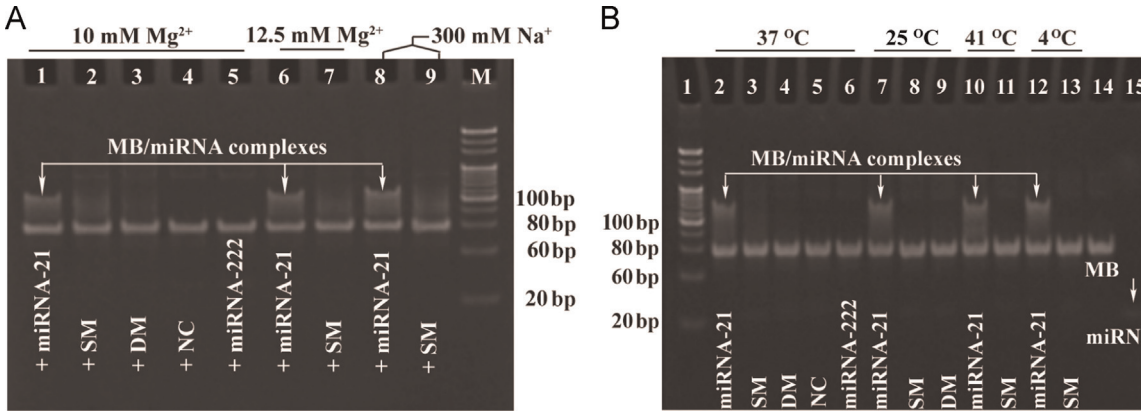

Fig. 5. PAGE analysis of the stringent affinity between MB and miRNA-21 as well as different spurious targets at different salt concentrations (37 °C) (A) and temperatures (10 mM Mg^{2+}) (B). (A) Lanes 1–5: 10 mM Mg^{2+}, lanes 6–7: 12.5 mM Mg^{2+}, lanes 8–9: 300 mM Na^{+}, and right lane: DNA size marker. (B) Lane 1: DNA size marker, lanes 2–6: 37 °C, lanes 7–9: 25 °C, lanes 10–11: 41 °C, lanes 12–13: 4 °C, lanes 14–15: negative control (MB and miRNA-21 only).

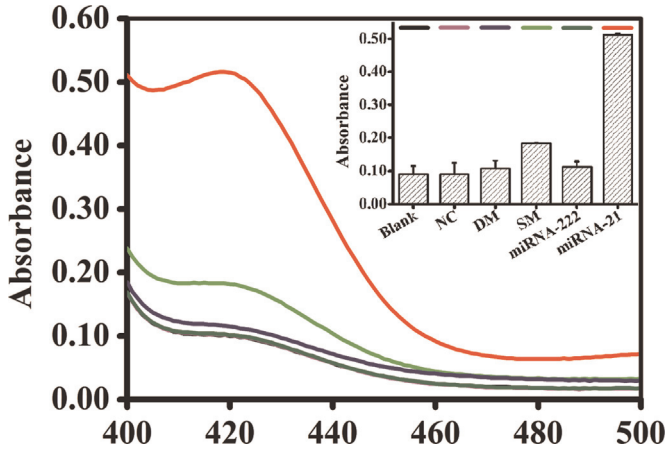

Fig. 6. Specificity of the assay to miRNA-21 (1 nM) over SM (2 nM), DM (2 nM), NC (2 nM) and mir-222 (2 nM). The error bars represent the standard deviations of measurements taken from three independent experiments.

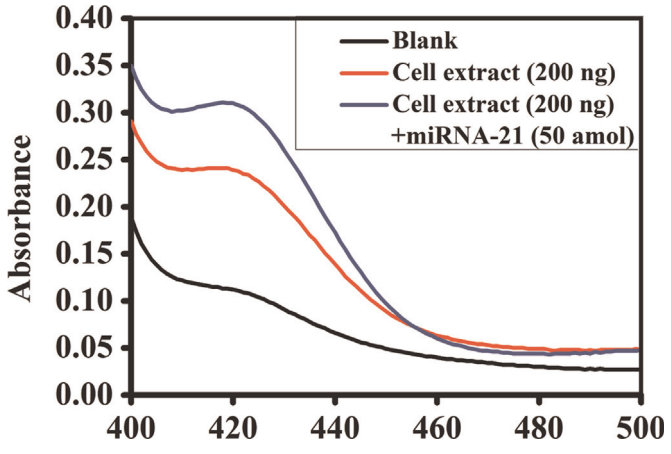

Fig. 7. UV-visable spectra of DNAzyme substrate mixed with the reaction mixtures obtained in absence and presence of total RNA from MCF-7 cells or miRNA-21.

machine was further investigated by measuring the absorbance of the proposed miRNA biosensing system for four types of miRNA sequences, including complementary target (miRNA-21), SM, DM, NC and miRNA-222 at 1.0, 2.0, 2.0, 2.0, and 2.0 nM, respectively. As shown in Fig. 6, the absorbance for SM, DM, NC and miRNA-222 was only 35.8%, 20.9%, 17.5% and 21.9% of that for miRNA-21, respectively. The high fidelity in discriminating perfectly complementary target and the mismatched strands or other miRNAs could be attributed to the high affinity and unique specificity of the smart modified MB. In addition, the reproducibility of the prepared biosensing system was also acceptable. Five replicate measurements of miRNA-21 at 100 fM and 10 pM showed the variation coefficients of 1.8% and 1.4%, respectively.

3.6. Real sample analysis

The proposed method could be successfully performed in real sample analysis using total RNA extracted from MCF-7 as an example. The total RNA was diluted to 400 ng/μL with DEPC-treated water, and 200 ng total RNA was used for detection. The absorbance generated by 200 ng of total RNA could be obviously distinguished from that generated by the blank (Fig. 7). From the calibration curve (Fig. 4B), the amount of miRNA-21 in 200 ng total RNA sample was estimated to be 97.5 amol (RSD=2.5%, $n=5$). To further evaluate its performance in real sample analysis and exclude the possible non-specific background signal, different amounts of miRNA-21 were spiked into 200 ng total RNA for the assay, and the results showed the recovery of 110–114% (Table 2), suggesting that the method could sensitively detect miRNA in real samples.

Table 2
Detection results of miRNA-21 spiked in extract from MCF-7 cells.

Samples	Concentration (pM)	Amount (amol)	Recovery (%)
Cell extract	2.00	97.5	
miRNA-21 (30 amol)	2.61	130.6	110
miRNA-21 (50 amol)	3.09	154.5	114
miRNA-21 (60 amol)	3.31	165.5	113
miRNA-21 (90 amol)	3.98	199.0	113

4. Conclusions

By taking advantage of cascade signal amplification with a modified MB mediated SDA multiple TIRCA, a functional nucleic acid-based amplification machine has been developed for an ultrasensitive visual detection of miRNA. The use of both passivated MB/GDNA probe and seal probe leads to stringently target recognition and specific signal amplification, which shows high sensitivity and can detect miRNA down to 5 aM with a with a dynamic range of 9 orders of magnitude. The designed methodology shows excellent specificity, good reproducibility, and acceptable accuracy for practical sample analysis. In addition, the whole process can be completed within 90 min. The developed

biosensing method provides a simple, rapid and sensitive platform for miRNA detection.

Acknowledgment

This work is supported by the National Basic Research Program (2010CB732400), National Natural Science Foundation of China (21135002, 81371904 and 81101638), Natural Science Foundation Project of CQ (CSTC2013jjB10019), and Research Fund for Post-graduate Innovation Project of Chongqing (Grant no. CYB14080).

References

[1] D.P. Bartel, Cell 116 (2004) 281–297.
[2] R.C. Lee, R.L. Feinbaum, V. Ambros, Cell 75 (1993) 843–854.
[3] Y. Liang, D. Ridzon, L. Wong, C. Chen, BMC Genom. 8 (2007) 166.
[4] S. Asaga, C. Kuo, T. Nguyen, M. Terpenning, A.E. Giuliano, D.S. Hoon, Clin. Chem. 57 (2011) 84–91.
[5] H.M. Heneghan, N. Miller, A.J. Lowery, K.J. Sweeney, J. Newell, M.J. Kerin, Ann. Surg. 251 (2010) 499–505.
[6] C. Li, Y. Feng, G. Coukos, L. Zhang, AAPS J. 11 (2009) 747–757.
[7] W. Zhu, W. Qin, U. Atasoy, E.R. Sauter, BMC Res. Notes 2 (2009) 89.
[8] J.A. Brito, C.C. Gomes, A.L. Guimaraes, K. Campos, R.S. Gomez, J. Oral Pathol. Med. 43 (2014) 211–216.
[9] W.C. Cho, Int. J. Biochem. Cell Biol 42 (2010) 1273–1281.
[10] J. Li, S. Tan, R. Kooger, C. Zhang, Y. Zhang, Chem. Soc. Rev. 43 (2014) 506–517.
[11] J. Stenvang, A.N. Silahtaroglu, M. Lindow, J. Elmen, S. Kauppinen, Semin. Cancer Biol. 18 (2008) 89–102.
[12] D. Duan, K.X. Zheng, Y. Shen, R. Cao, L. Jiang, Z. Lu, J. Li, Nucleic Acids Res. 39 (2011) e154.
[13] R.K. Saiki, S. Scharf, F. Faloona, K.B. Mullis, G.T. Horn, H.A. Erlich, Science 230 (1985) 1350–1354.
[14] A. Valoczi, C. Hornyik, N. Varga, J. Burgyan, S. Kauppinen, Z. Havelda, Nucleic Acids Res. 32 (2004) e175.
[15] C. Chen, D.A. Ridzon, A.J. Broomer, Z. Zhou, D.H. Lee, J.T. Nguyen, Nucleic Acids Res. 33 (2005) e179.
[16] E.M. Kroh, R.K. Parkin, P.S. Mitchell, M. Tewari, Methods 50 (2010) 298–301.
[17] S. Bi, Y. Cui, L. Li, Anal. Chim. Acta 760 (2013) 69–74.
[18] H.F. Dong, S. Jin, H.X. Ju, K.H. Hao, L.P. Xu, H.T. Lu, Anal. Chem. 84 (2012) 8670–8674.
[19] Y. Wen, Y. Xu, X. Mao, Y. Wei, H. Song, N. Chen, Anal. Chem. 84 (2012) 7664–7669.
[20] S. Bi, L. Li, Y.Y. Cui, Chem. Commun. 48 (2012) 1018–1020.
[21] M. Wang, Z. Fu, B. Li, Y. Zhou, H. Yin, S. Ai, Anal. Chem. 86 (2014) 5606–5610.
[22] Y.Q. Liu, M. Zhang, B.C. Yin, B.C. Ye, Anal. Chem. 84 (2012) 5165–5169.
[23] S. Bi, Y. Cui, Y. Dong, N. Zhang, Biosens. Bioelectron. 53 (2014) 207–213.
[24] Y.Q. Cheng, X. Zhang, Z.P. Li, X.X. Jiao, Y.C. Wang, Y.L. Zhang, Angew. Chem. Int. Ed. 48 (2009) 3268–3272.
[25] L. Cui, Z. Zhu, N.H. Lin, H.M. Zhang, Z.C. Guan, C.Y. Yang, Chem. Commun. 50 (2014) 1576–1578.
[26] R. Deng, L. Tang, Q. Tian, Y. Wang, L. Lin, J. Li, Angew. Chem. Int. Ed. 53 (2014) 2389–2393.
[27] H.Y. Liu, L. Li, L.L. Duan, X. Wang, Y.X. Xie, L.L. Tong, Q. Wang, Anal. Chem. 85 (2013) 7941–7947.
[28] Y.T. Zhou, Q. Huang, J.M. Gao, J.X. Lu, X.Z. Shen, C.H. Fan, Nucleic Acids Res. 38 (2010) e156.
[29] Y. Huang, J. Chen, S. Zhao, M. Shi, Z.F. Chen, H. Liang, Anal. Chem. 85 (2013) 4423–4430.
[30] C. Zong, J. Wu, M.M. Liu, L.L. Yang, F. Yan, H.X. Ju, Anal. Chem. 86 (2014) 9939–9944.
[31] M. Shi, S.L. Zhao, Y. Huang, L.M. Zhao, Y.M. Liu, Talanta 124 (2014) 14–20.
[32] H.X. Jia, Z.P. Li, C.H. Liu, Y.Q. Cheng, Angew. Chem. Int. Ed. 49 (2010) 5498–5501.
[33] C.Y. Yan, C. Jiang, R.Q. Yu, Anal. Sci. 29 (2013) 605–610.